LAWRENCE
LIVERMORE
NATIONAL
LABORATORY

Density Effects on Tokamak Edge Turbulence and Transport with Magnetic X-points

X. Q. Xu, R. H. Cohen, W. M. Nevins, T. D. Rognlien, D. D. Ryutov, M. V. Umansky, L. D. Pearlstein, R. H. Bulmer, D. A. Russell, J. R. Myra, D. A. D'Ippolito, M. Greewald, P. B. Snyder, M. A. Mahdavi

Disclaimer

Density Effects on Tokamak Edge Turbulence and Transport with Magnetic X-points[1]

X.Q. Xu 1), R.H. Cohen 1), W.M. Nevins 1), T.D. Rognlien 1), D.D. Ryutov 1),
M.V. Umansky 1), L.D. Pearlstein 1), R.H. Bulmer 1), D.A. Russell 2), J.R. Myra 2),
D.A. D'Ippolito 2), M. Greenwald 3), P.B. Snyder 4), M.A. Mahdavi 4)

1) Lawrence Livermore National Laboratory, Livermore, CA 94551 USA
2) Lodestar Research Corporation, Boulder, CO 80301 USA
3) MIT Plasma Science & Fusion Center, Cambridge, MA 02139 USA
4) General Atomics, San Diego, CA 92186 USA

e-mail contact of main author: xxu@llnl.gov

Abstract. Results are presented from the 3D electromagnetic turbulence code BOUT, the 2D transport code UEDGE, and theoretical analysis of boundary turbulence and transport in a real divertor-plasma geometry and its relationship to the density limit. Key results include: (1) a transition of the boundary turbulence from resistive X-point to resistive-ballooning as a critical plasma density is exceeded; (2) formation of an X-point MARFE in 2D UEDGE transport simulations for increasing outboard radial transport as found by BOUT for increasing density; (3) formation of a density pedestal due to neutral fueling; (4) identification of convective transport by localized plasma "blobs" in the SOL at high density and decorrelation of turbulence between the midplane and the divertor leg due to strong X-point magnetic shear; (5) a new divertor-leg instability driven by a radial tilt of the divertor plate.

1. Introduction

Achieving high energy confinement at high density is important since the fusion power increases with density as $P_{FUS} \propto n^2 \langle \sigma v \rangle$, where n is the ion density and $\langle \sigma v \rangle$ is the fusion reaction rate. However, the empirical Greenwald scaling shows that the maximum attainable tokamak plasma density (n_G) is proportional to plasma current, which in turn is limited by MHD kink instabilities [1]. While density limits have been observed for several decades, there is no widely accepted first-principles theory available. Though the empirical scaling is expressed in terms of the line-averaged electron density, the various experiments suggest that it is an edge phenomenon and that the observed density limit is the result of rapid edge cooling [1].

In this paper, we present a series of studies related to density effects on tokamak edge turbulence and related transport with magnetic X-points [2]. The simulations were carried out primarily using the fluid 3D turbulence code BOUT and the coupled turbulence and transport BOUT-UEDGE codes [3]. BOUT is a 3D non-local electromagnetic fluid turbulence simulation code and has recently been updated to include a neutral particle source. The plasma transport is self-consistently driven by boundary turbulence, while neutrals are described

by a simple analytic model. The plasma profiles are evolved simultaneously with the turbulence in the presence of a prescribed heat source from the core plasma and the particle source from the neutrals. The coupled code BOUT-UEDGE has been developed to simulate very slow physics process in the edge region, such as particle recycling. For toroidally symmetric transport with model cross-field diffusion coefficients, BOUT has been benchmarked with the 2D transport code UEDGE without neutrals. BOUT simulations demonstrate that boundary turbulence undergoes a transition from resistive X-point to resistive-ballooning and enhanced radial transport is observed as a critical plasma density is exceeded [2]. The result suggests that large radial transport is a key process for rapid edge cooling which leads to the tokamak density limit.

The possible presence of a strong instability in the divertor legs, totally decoupled from the main scrape-off layer (SOL), is of significant practical importance, because one may then hope that, for long-enough legs, the transport produced by this instability would reduce the divertor heat load without having any direct impact on the main SOL, and therefore not lead to the degradation of confinement of the core plasma. In this context, we have considered effect of a finite plasma beta on the divertor-leg instability and have found that, at high-enough betas, there exist modes evanescent along the field lines and therefore not reaching the X-point region. These modes are perfectly uncoupled from the main SOL and are a desirable ingredient of divertor design. We have found that these modes are enhanced by proper tilt of the divertor plate: "outward" tilt in the common flux region, and "inward" tilt in the private flux region.

The paper is organized as follows: The changing character of turbulence for increasing density is described in Sec. 2. Self-consistent turbulence and transport simulations with a neutral source added is presented in Sec. 3, including blob dynamics and correlation analysis. Section 4 analyzes the divertor-leg instability. The long-time BOUT-UEDGE coupling is described in Sec. 5. The conclusions are given in Sec. 6.

2. Changing turbulence character with increasing density

A series of BOUT simulations has been conducted to investigate the physical processes which limit the density in tokamak plasmas [2]. In this section, the plasma profiles are frozen, while they are evolved in sections 3 and 4. The background magnetic field structure is obtained from an MHD equilibrium code (*e.g.*, EFIT [4]) for a typical shot. The plasma profiles of density and electron temperature are analytic fits (modified tanh) to Thomson scattering data. For scaling studies with plasma density, the plasma pressure is held constant. For scaling studies with plasma current, the background magnetic field structure is obtained from the MHD equilibrium code Corsica [5]. Simulations of turbulence in tokamak boundary plasmas show that turbulent fluctuation levels and transport increase with collisionality. At high edge density, perpendicular turbulent transport dominates parallel classical transport, leading to substantially reduced contact with divertor plates and the destruction of the $\mathbf{E} \times \mathbf{B}$ edge shear layer, and the region of high transport then extends inside the last closed magnetic flux surface. As the density increases, these simulations show that the resistive X-point mode transitions to the resistive ballooning mode.

The corresponding root-mean-squared (rms) radial-poloidal mode structures are shown in Fig. 1a for three different background densities: $\overline{n}_e = 0.28 n_G$, $\overline{n}_e = 0.56 n_G$, and $\overline{n}_e = 1.12 n_G$.

Here $\overline{n}_e$ is the line-averaged density in $10^{20}m^{-3}$, $n_G = I_p/\pi a^2$ in $10^{20}m^{-3}$. For the bottom base case which corresponds to a DIII-D L-mode experiment, $I_p = 0.974$MA, $a = 0.59$m and $\overline{n}_e = 0.25 \times 10^{20}m^{-3}$. The typical resistive X-point mode appears at the bottom of the plot
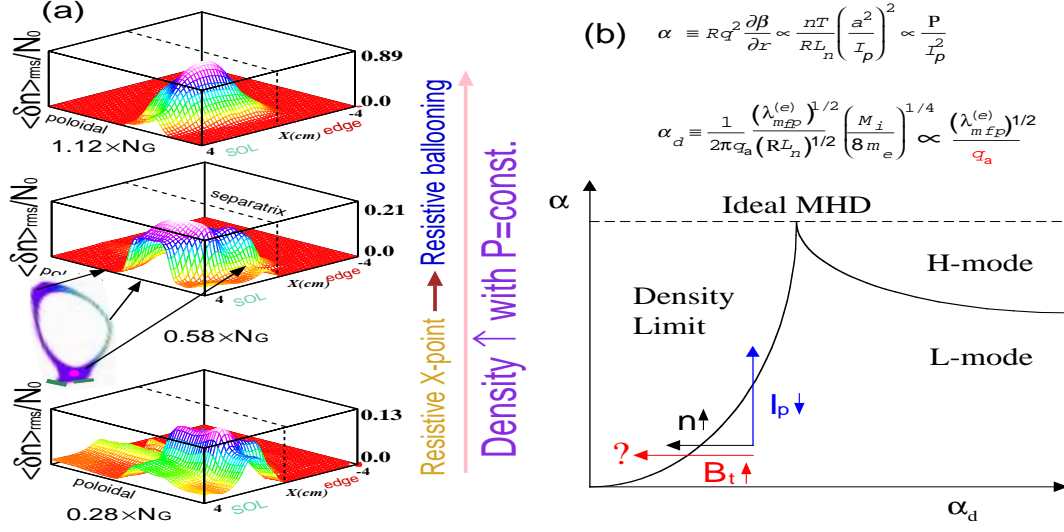

FIG. 1: (a). The rms levels of the radial-poloidal profiles of fluctuation density calculated from BOUT simulation. As the Greenwald density limit is approached or exceeded, the SOL density fluctuation increases and peaks around the outer midplane. Here $N_0 = 1.2 \times 10^{19}/m^3$. (b). A sketch of edge plasma phase space from Rogers, Drake and Zeiler Theory [6].

as a base case. In this regime, the X-point effects are the most dramatic. The eigenfunction illustrates that resistivity is dominant near the X-points, allowing the mode to decrease rapidly away from this region. As density increases, moving vertically up from the bottom of the plot, the rms fluctuation levels increase dramatically, and the modes are poloidally peaked around the outer midplane. For fixed pressure, as density increases, the temperature decreases, and one enters the strong resistive ballooning regime in the top of the plot. In this case, ballooning of the eigenfunction at the outboard midplane reduces the importance of X-point effects, and it becomes a classical resistive MHD mode. These results clearly demonstrate the transition from resistive X-point mode to resistive ballooning mode as the density approaches and exceeds the Greenwald density.

A set of 2D UEDGE transport simulations with increasing outboard convective radial transport as found by BOUT for increasing density, shows that this transport can lead to an X-point MARFE when a fixed-fraction carbon impurity radiation is included [2]. This is a common symptom of density-limit related disruptions. BOUT further demonstrates that the current scaling appears on a plot of discharge current versus density as abruptly large radial transport once the Greenwald density is approached or exceeded. All of these results indicate that rapid edge cooling due to large radial transport is a key physics element of the tokamak density limit. The simulation results are qualitatively consistent with experimental observations from C-mod and DIII-D.

These simulations are qualitatively consistent with previous theory and simulations given by Rogers, Drake and Zeiler (RDZ) [6], with the exception of the q-dependence in their α_d scaling. The three sets of simulations are extrapolated to compare with RDZ theory and experiments, and to check whether a density limit boundary line is crossed, as the arrows

indicate in Fig. 1b. (1). For fixed safety factor q, current I_p and pressure P, an increase in density n_e leads to a fixed α and a decrease in α_d, $\alpha_d \propto \sqrt{\lambda^e_{mfp}} \propto 1/\sqrt{n_e}$. In this case, the density-limit boundary is crossed, and theory, BOUT simulations and experiments agree. (2). For fixed q, temperatures T_e, T_i and density n_e, a decrease in current I_p leads to an increase in $\alpha \approx 1/I_p^2$ and constant α_d. In this case, the density limit boundary is crossed, and theory, BOUT simulations and experiments agree. (3). For fixed I_p, T_e, T_i and n_e, an increase in toroidal magnetic field B_t leads to a fixed α and a decrease in $\alpha_d \approx 1/q$ since $q \propto B_t$. In this case, the RDZ theory predicts a density limit, but both experiments [7] and BOUT find no transition for this case. The disagreement may be due to two important pieces of physics omitted from RDZ theory that are kept in BOUT simulations: X-point physics and Scrape-Off-Layer (SOL) physics. X-point physics limits the mode to the outside midplane such that the parallel connection length qR is not a good measure of the parallel mode width. SOL physics contributes significantly to the formation of E_r well and our simulations show that the onset of large radial transport is associated with the destruction of the $\mathbf{E} \times \mathbf{B}$ edge shear layer.

3. Blob dynamics and density pedestal

For self-consistent turbulence and transport simulations with a neutral source added, we find that as density rises due to neutral fueling, turbulence transport increases. The same trend has been obtained with fixed plasma profiles as discussed in last section. The characteristics of the fluctuations also changed from small scale turbulence to large density structures called blobs. At high density during density ramp-up simulations, we have identified convective transport by localized plasma "blobs" in the SOL of a 3D BOUT simulation [10]. These
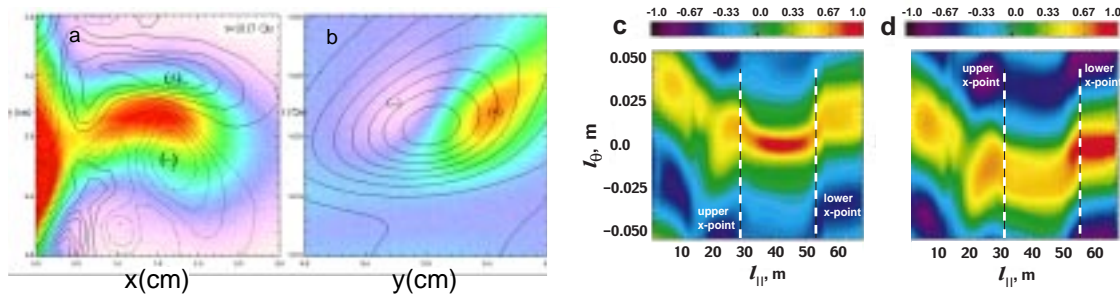

FIG. 2: (a). Blob detached from the separatrix, vorticity over density (color); (b). History of blob vorticity at the wall, density over vorticity (color); (c). Correlation function for reference point at outer midplane (d). Correlation function for reference point at outer divertor leg.

properties include: (1) Blob detachment from the separatrix: spatially localized and non-diffusive transport of positive density fluctuations radially outward, as shown in Fig. 2a. (2) Blob translation from dipole vorticity with the $\mathbf{E} \times \mathbf{B}$ drift calculated from potential fluctuations, as shown in Fig. 2b. The self-consistent E-field of the blob is predominantly a dipole field, increasingly as the blob moves away from the separatrix. The radial velocity appears to scale as $1/a_{eff}^2$ [12], where a_{eff} is blob radius. (3) Blob rotation (monopole vorticity): observed to decay, probably due to T_e relaxation and/or sheath disconnection. (4) Cross Correlation analysis indicates a decorrelation of turbulence between the midplane and the divertor leg due to strong X-point magnetic shear [13]. Figure 2c shows that the cross-correlation has cutoffs near both the lower X-point and the upper X-point regions for reference point at outer midplane, and the cutoff is more pronounced for larger poloidal

wavenumber k_θ. Figure 2d shows that the cross-correlation has cutoffs near the X-point regions for reference point at outer divertor leg. It is also shown in Fig. 2c and 2d that the poloidal correlation length is about 1 cm and the parallel correlation length is about 20 meters.
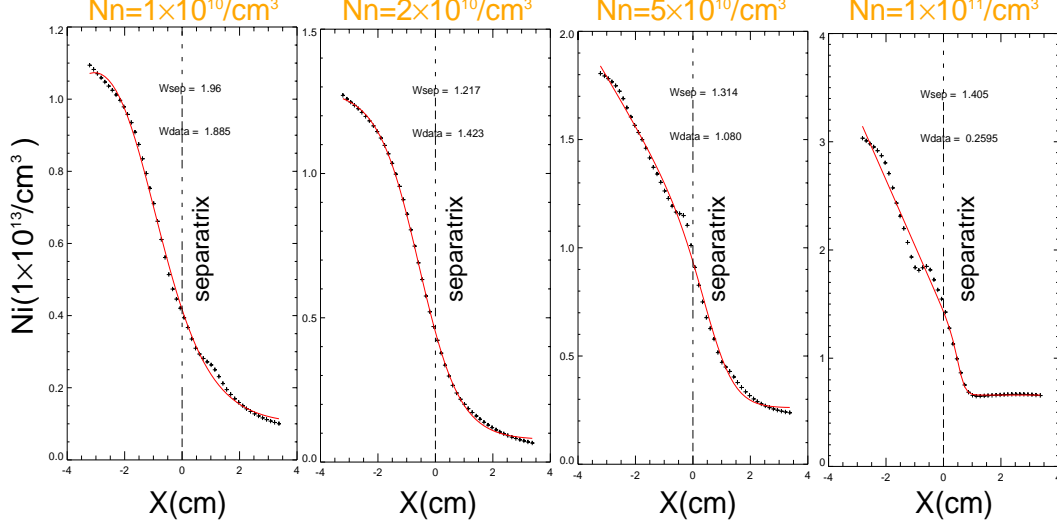

FIG. 3: *Background plasma density and its modified tanhfit to the simulation profiles after* ~ 0.5–$1ms$ *evolution vs.neutral density at the outside midplane*

The simulation results also show that the formation of a density pedestal around the separatrix in L-mode even though the calculated plasma diffusion coefficients are almost radially constant and there is no temperature pedestal [8]. The simulation data points with different neutral density at the wall and their fit to a "modified tanhfit" formula [8] are plotted in Fig. 3. The density gradient scale length parameters are obtained by fitting the modified tanhfit function to these profiles. There is a general overall trend of the minimum density gradient scale length W_{data} to decrease with increasing pedestal density as observed in the experimental data [9]. However, the center position of the modified tanhfit is moving toward the SOL and the modified tanhfit is no longer the best fit, due to the appearance of large blob structures as the density increases. It is also shown that the density gradient scale length at the separatrix W_{sep} is roughly constant with increasing pedestal density.

4. Long-time turbulence/profile evolution

As shown above, the turbulence code can evolve profiles over times on the order of 1 ms, which is comparable to the ion transit time from midplane to divertor plate near the separatrix. However, near-unity particle recycling and sputtering from the divertor plates and walls results in edge plasma profile evolution that typically has a time-scale in excess of 10 ms. To treat such long profile evolution, a scheme [17] has be implement that iteratively couples BOUT turbulence to the 2D axisymmetric UEDGE transport code. For example, the continuity equation for the ion density n_i is separated into two equations, one describing the long-time evolution of the temporally- and toroidally-averaged density, $N_i \equiv \langle n_i \rangle_{\phi,t}$, and the second giving the rapidly varying fluctuations $\tilde{n}_i \equiv n_i - N_i$, yielding

$$\partial_t N_i + \nabla \cdot \langle \Gamma \rangle = \langle S \rangle \;\; \text{and} \;\; \partial_t \tilde{n}_i + \nabla \cdot (\Gamma - \langle \Gamma \rangle) = S - \langle S \rangle. \tag{1}$$

The radial particle flux, Γ_r, has a large turbulence-induced component provided by the BOUT code in the form $\langle \Gamma_r \rangle = \langle \tilde{n}_i \tilde{v}_r \rangle$, and the turbulence code in turn receives the detailed profile information for N_i from UEDGE that provides a consistent model of neutral sources from divertor and wall recycling. This procedure is efficient compared to straightforward evolution of the full 3D system because a substantial time-scale separation exists in the edge (~ 0.1 ms for saturation of turbulence and > 10 ms for transport). We focus on a self-consistent statistical steady-state by running each code on its own characteristic time-scale. For numerical stability, a relaxation iteration is used where only a fraction of new plasma fluxes and profile changes are updated on each iteration [17].

The iterative procedure has been used for 4 plasma variables (n_i, $v_{i\parallel}$, T_e, and T_i) and has produced approximate steady-states after ~ 10 iterations [3]. The neutral recycling model from UEDGE produces plasma profiles in both the radial and poloidal directions (a low temperature, high density divertor region), thus include self-consistent profiles of the type examined in Sec. 3 These cases have no E_r well, and thus correspond to the situation where the turbulence has destroyed the well. Both codes have axisymmetric E_r models available, and work is underway obtain a unified description.

An example of the turbulence/transport coupling is illustrated in Fig. 5a where the iteration history of the midplane density is shown for a DIII-D single-null configuration with ~ 2 MW input. The full 2D contour of the effective radial diffusion coefficient after the final 9th iteration is shown in Fig. 5b.. Note that the turbulent flux, which has a strong outward convective character in the SOL, can sometimes be represented by a spatially dependent diffusion coefficient as done here. More generally, we use both diffusive and convective terms to match the fluxes. Here the strong ballooning character of the turbulence is very evident.

These cases do show strong plasma fluxes to the main chamber wall, with typically $\sim 30\%$ going to such walls compared to the divertor plates, Nevertheless, owing to the the smaller surface area of the divertor footprint, the density and local H_α intensity there is very much larger than at the walls. Also, these simulations assume a wall conformal to the poloidal magnetic flux surface with a value of 1.1 normalized to the separatrix value; in reality, the wall can be significantly farther away at many toroidal and poloidal positions.
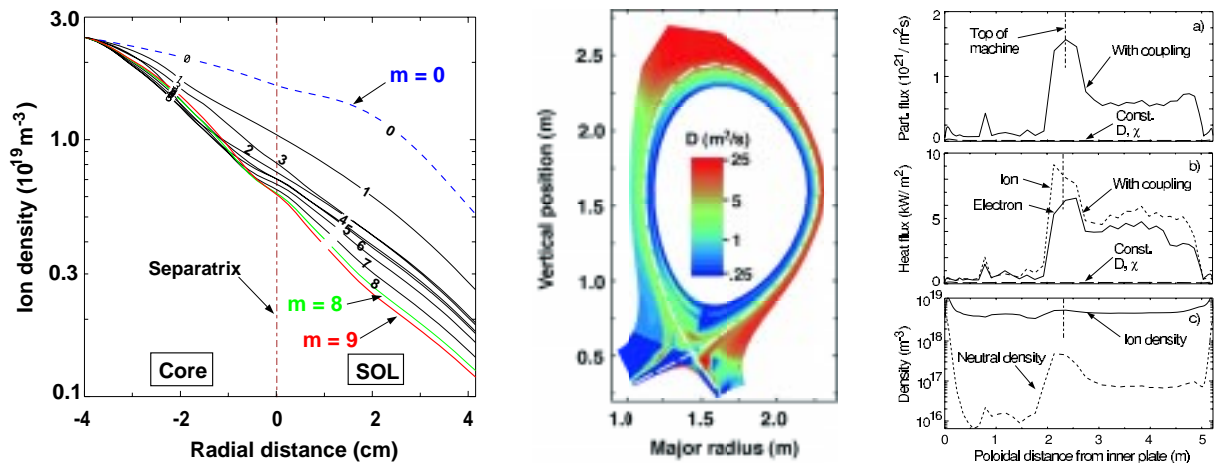

FIG. 4: Left panel: iteration history (m=index) of midplane density for BOUT/UEDGE coupling. Middle panel: effective radial turbulent particle diffusivity after the m=9 iteration. Right panel: particle fluxes to chamber wall after the m=9 iteration with ion and neutral density

5. Finite-beta modes localized near the divertor plate

We consider the slab geometry shown in Fig. 4a. To visualize the instability in the clearest way, we assume that the only unperturbed quantity that has spatial variation is the electron temperature, $T_e = T_e(x)$. The other unperturbed quantities are assumed to be uniform both in the radial and poloidal directions. We consider the case of low recycling, where the plasma approaching the divertor plate is not perturbed by the neutrals formed on the plate. The plasma flows towards the divertor plate with parallel velocity u exceeding the sound speed.

The unstable mode does not reach the X point if the growth rate is large enough, $Im\Omega > v_A/L$, where L is the characteristic distance from the plate to the X point, and v_A is the Alfven velocity. We make this assumption, derive the dispersion relation, and then determine the parameter domain where the assumption $Im\Omega > v_A/L$ is valid. The mode we find is an evanescent Alfvèn mode. We consider perturbations with $k_x\Delta > 1$, $k_y >> k_x$ (here $\Delta = |T_e/T_e'|$ is the length-scale of the radial temperature variation). We also assume that $k_y\rho_i \ll 1$, so that one can use a gyrofluid approach ($\rho_i = \omega_{ci}^{-1}\sqrt{2T_i/m_i}$ is the ion gyroradius) . Then, we impose sheath boundary conditions on the divertor plate, analogous to those described in [15, 16]. This gives rise to the following dispersion relation:

$$\Omega\left[i\left(v_A + \frac{\omega_{ci}^2 m_i u}{k_y^2 T_e}\right) + \frac{\omega_{ci}}{k}\frac{B_z}{B_y}\tan\alpha\right] = \frac{T_e'}{T_e}\left[i(\Lambda + 0.5)\frac{\omega_{ci}u}{k} + \frac{T_e}{m_i}\tan\alpha\right] = 0. \quad (2)$$

where Λ is a logarithm of the ratio of the electron and ion thermal velocities. On Fig. 4b, we plot the normalized growth rate $Im\tilde{\Omega} = (L/v_A)Im\Omega$ vs. the normalized wave-number $\tilde{k} = k_y\rho_i$. We assume that $T_e'\tan\alpha < 0$, i.e., the temperature decreasing in the outward direction, and the plate tilted as shown on Fig. 4a. The results show that "outward" tilt
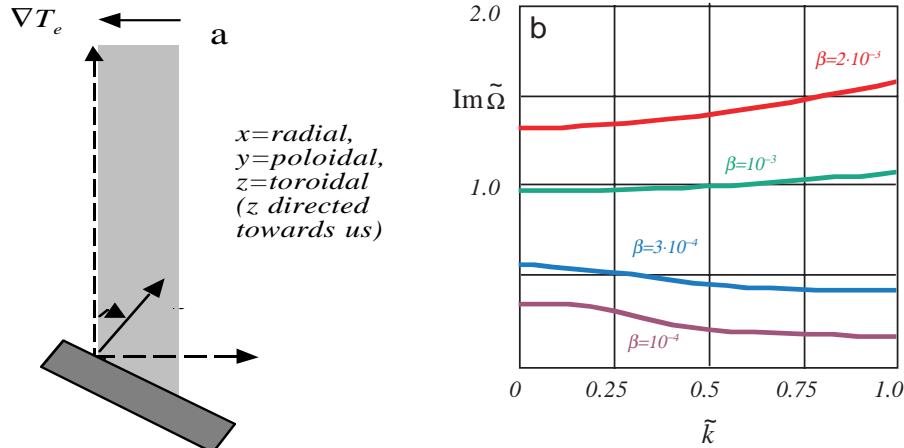

FIG. 5: (a). The geometry of the problem. The X=0 plane corresponds to the separatrix. The common flux region is shown. The private flux corresponds to $x, 0$. (b). Normalized growth rate vs normalized wave number. Assumptions about the plasma parameters are $T_e = T_i = T; v\| = 2\sqrt{2T/m}; B_z/B_y = 5; \Lambda = 2.5, L/\Delta = 500, \tan\alpha = 10$. The mode localized in the divertor leg exists only if $Im\tilde{\Omega} > 1$. This condition sets the range for β and k where our analysis is consistent. In particular, for $\beta = 10^{-4}$, there are no localized modes at any wavenumber.

(as on Fig. 4a) increases the instability. As is clear from Eq. (1), the instability is absent in the case of no tilt. The physical mechanism for that is largely related to the additional force acting on the flux tube displaced along the surface of the tilted plate [14, 15]. Fig. 4b shows

that the localized mode exists only if the plasma beta is high enough. For the parameters chosen for Fig. 4b, beta must be higher than 10^{-3}.

6.   Summary and conclusions

This paper presents recent analyses of density effects on tokamak turbulence and transport with X-points. These unique comprehensive studies are based on edge turbulence and impurity transport from BOUT and UEDGE simulations, and analytic theory with X-points. The results are new and significant. We show that as density rises, the fluctuation is changed from resistive X-point mode to resistive ballooning mode, from small scale turbulence to large blobs. In the large blob regime at high density, the enhanced radial transport as shown is likely to lead to rapid edge cooling, which leads to the density limit. The description given here is consistent with recent experiments on C-Mod [18]. Our theoretical analysis find a new divertor-leg instability in the finite beta regime due to a radial tilt of the divertor plate. This instability would produce transport that reduces the divertor heat load while having no direct impact on the upper SOL. In summary, our results are helpful in shedding light on the qualitative trend and scalings, and provide suggestions of possible experimental control techniques. The successful development of the coupling of the BOUT and UEDGE codes offers a state-of-the-art edge fluid simulation capability, self-consistently including turbulence, transport, neutrals and impurities.

References

[1] GREENWALD, M., TERRY, J.L., *et al.* Nucl. Fusion **28** (1988) 2199.

[2] XU, X.Q., NEVINS, W.M., *et al.* Phys. Plasmas **10** (2003) 1773.

[3] ROGNLIEN, T.D., UMANKSKY, M.V., *et al.* Contrib. Plasma Phys. **44** (2004) 188; also J. Nucl. Mater., accepted (2004).

[4] LAO, L.L., ST. JOHN, H,. *et al.* Nucl. Fusion **25** (1985) 1611.

[5] PEARLSTEIN, L.D., BULMER, R.H. *et al.* Proc. 28th EPS Conf. Controlled Fusion Plasma Phys, Madeira, Portugal, June 2001, (EPS, Funchal, 2001), Vol. 25A (ECA), p. 1901; http://www.cfn.ist.utl.pt/EPS2001/fin/authors/nav/AutP01fr.html

[6] ROGERS, B.N., DRAKE, J.F., *et al.* Phys. Rev. Lett. **81** (1998) 4396.

[7] PETRIE, T.W., KELLMAN, A.G., *et al.* Nucl. Fusion **33** (1993) 929.

[8] XU, X.Q., NEVINS,W.M., *et al.*, Contr. Plasma Phys. **44** (2004) 105.

[9] GROEBNER, R.J., MAHDAVI, M.A., *et al.* 19th IAEA Fusion Energy Conference (Lyon, France, 14 to 19 October 2002), IAEA-CN-94/EX/C2-3.

[10] RUSSELL, D.A., D'IPPOLITO, D.A., *et al.*, submitted, Phys. Rev. Lett. (2004).

[11] KRASHENINNIKOV, S.I., Phys. Lett. A **283** (2001) 368.

[12] D'IPPOLITO, D.A., MYRA, J.R., *et al.*, Phys. Plasmas **9** (2002) 222; also this conf.

[13] UMANSKY, M.V., ROGNLIEN, T.D., *et al.*, Contr. Plasma Phys. **44** (2004) 182.

[14] RYUTOV, D.D, and COHEN, R.H., Contr. Plasma Phys. **44** (2004) 168.

[15] FARINA, D., POZZOLI, R., Plasma Phys. Contr. Fusion, 35, 1271 (1993).

[16] COHEN, R. H., RYUTOV, D. D., Phys. Plasmas, 2, 2011 (1995).

[17] SHESTAKOV, A.I., COHEN, R.H., *et al.*, J. Comp. Phys. **185**, 399 (2003).

[18] TERRY, J.L., ZWEBEN, S. J., *et al.*, Phys. Plasmas, 10, 1739 (2003), Jerry, T. L., also this conf.